EUROfusion

Impact of supra-thermal particles on plasma performances at ASDEX Upgrade with GENE-Tango simulations

A. Di Siena[1], R. Bilato[1], A. Banon. Navarro[1], M. Bergmann[1], L. Leppin[1], T. Görler[1], E. Poli[1], M. Weiland[1], G. Tardini[1], F. Jenko[1], The ASDEX Upgrade Team[1,2] and the EUROfusion MST1 Team[3]

[1] Max Planck Institute for Plasma Physics, Boltzmannstr. 2, 85748 Garching, Germany

[2] Stroth et al 2022 (https://doi.org/10.1088/1741-4326/ac207f)

[3] Labit et al 2019 (https://doi.org/10.1088/1741-4326/ab2211)

IPP

This work has been carried out within the framework of the EUROfusion Consortium, funded by the European Union via the Euratom Research and Training Programme (Grant Agreement No 101052200 — EUROfusion). Views and opinions expressed are however those of the author(s) only and do not necessarily reflect those of the European Union or the European Commission.

Motivation

Main goal

Prediction of plasma profile evolution in advanced tokamak scenarios **with significant fast-ion content** up to transport time-scale.

Relevance

- Fast particles strongly suppress turbulent transport in experiments and simulations → **new pathways to scenario optimisation**.
- Supra-thermal particle effects on turbulence not fully captured by reduced models, e.g., TGLF.

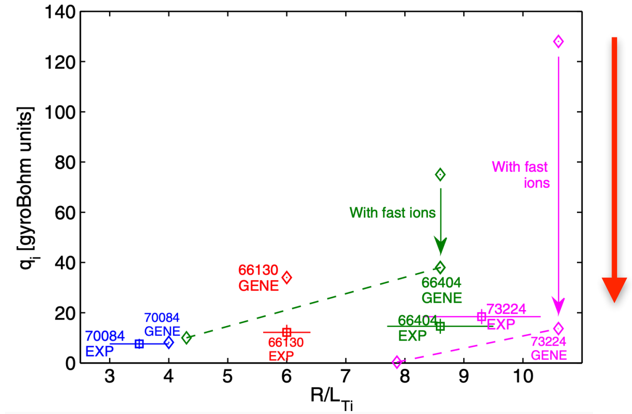

J. Citrin et al. PRL 2013

Motivation

Main goal

Prediction of plasma profile evolution in advanced tokamak scenarios **with significant fast-ion content** up to transport time-scale.

Relevance

- Fast particles strongly suppress turbulent transport in experiments and simulations → **new pathways to scenario optimisation**.
- Supra-thermal particle effects on turbulence not fully captured by reduced models, e.g., TGLF.

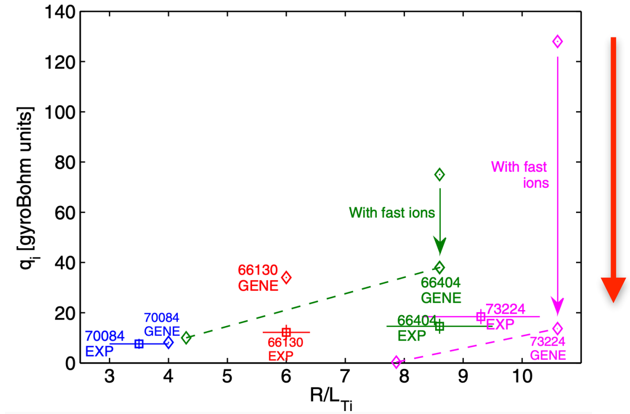

J. Citrin et al. PRL 2013

Our contribution:

- Fast ion studies limited only to micro-turbulence time-scale → how do they impact thermal profiles?
- Are fast ion modes a limiting factor for the T_i-peaking or are they one of the main cause?

Limits of previous work

Current status

- Fast ion induced nonlinear stabilization effects on turbulence studied only on micro-turbulence time scales → plasma profiles and magnetic geometry fixed.

Technical limitations to study fast ion effects on confinement time

- Separation between transport ($\tilde{t}$) and turbulence (t) time scales is $\tilde{t}/t \sim (a/\rho)^2$.
- Simulations to confinement time are expensive: feasible for small machines (TCV: $a/\rho < 100$), prohibitive for large experiments (ITER: $a/\rho \sim 1000$).

Computational cost $> (a/\rho)^3 \rightarrow$

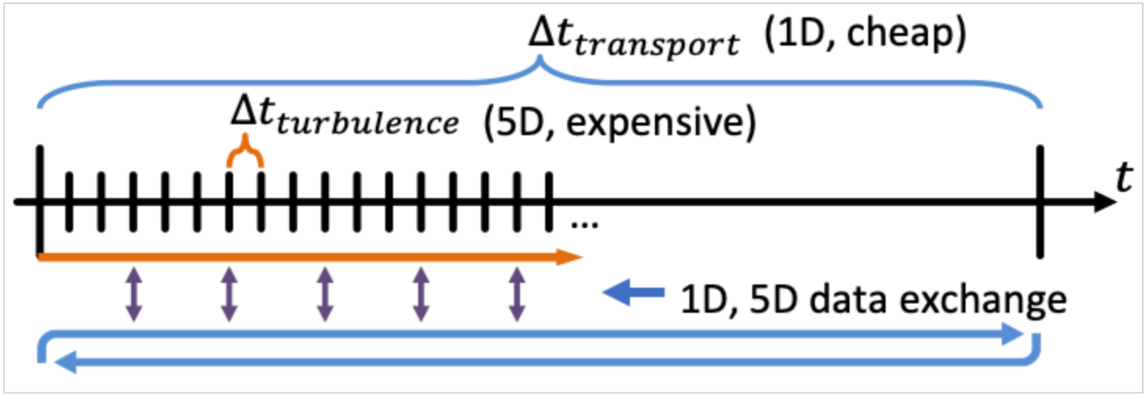

Limits of previous work

Current status

- Fast ion induced nonlinear stabilization effects on turbulence studied only on micro-turbulence time scales → plasma profiles and magnetic geometry fixed.

Technical limitations to study fast ion effects on confinement time

- Separation between transport ($\tilde{t}$) and turbulence (t) time scales is $\tilde{t}/t \sim (a/\rho)^2$.
- Simulations to confinement time are expensive: feasible for small machines (TCV: $a/\rho < 100$), prohibitive for large experiments (ITER: $a/\rho \sim 1000$).

Computational cost $> (a/\rho)^3 \rightarrow$

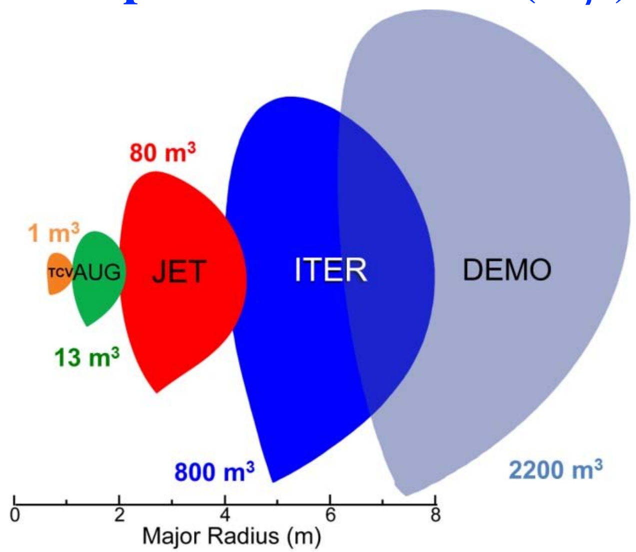

Bringing gyrokinetic simulations to transport time scale

GENE-Tango coupling

(i) GENE evaluates turbulence levels for given pressure profile

(ii) Tango evaluates new plasma profiles consistent with given turbulence levels and experimental sources.

(iii) New profiles transferred back to GENE and the process is repeated.

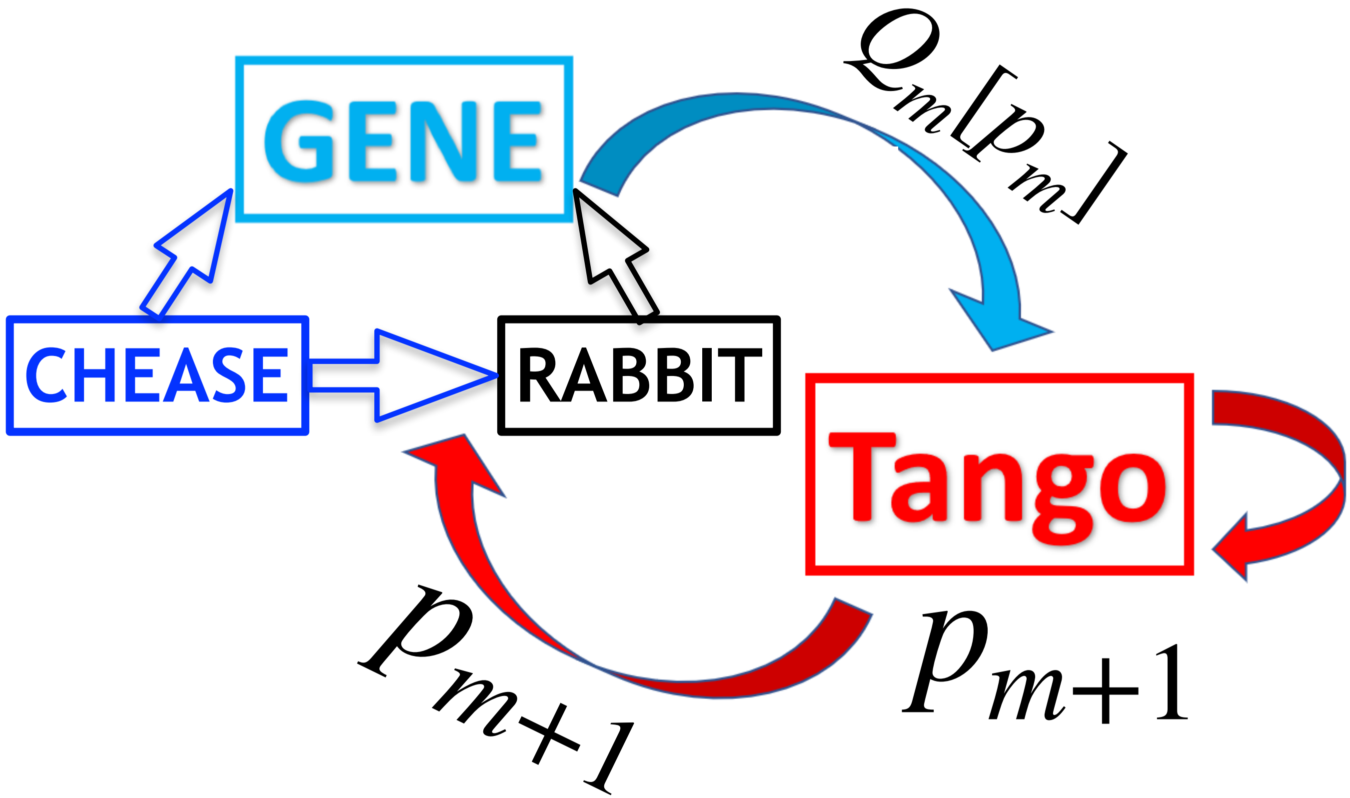

ASDEX Upgrade 39230 @ t = 2.7 s - TGLF-ASTRA

- ASDEX Upgrade #39230 at t = 2.7s; large NBI power and localized ECRH.

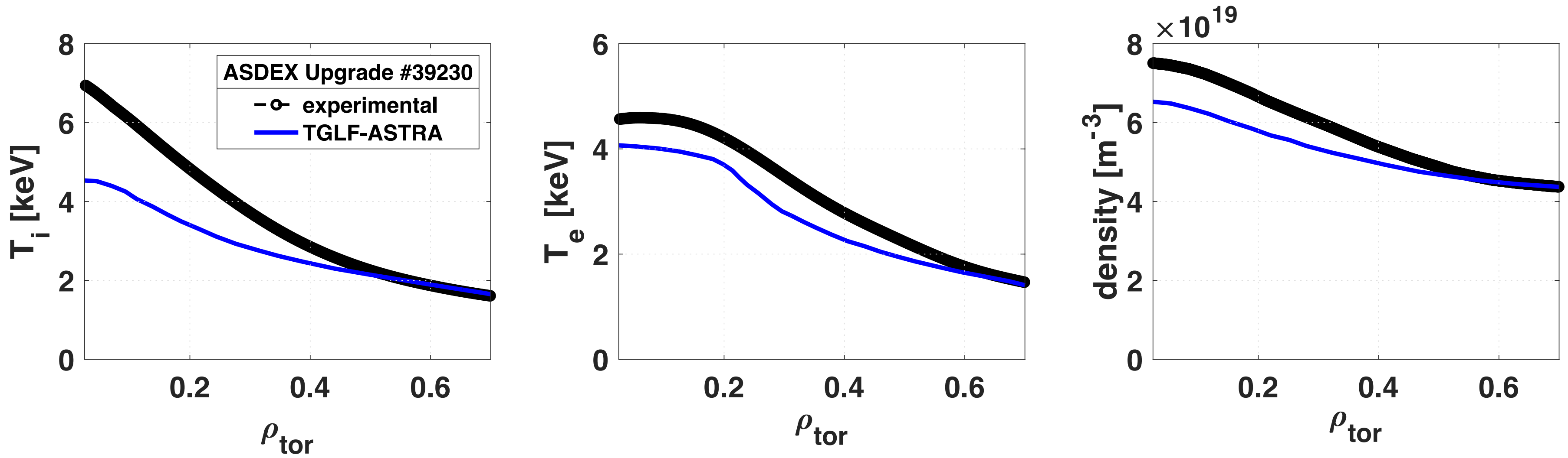

- Poor matching of TGLF-ASTRA on the experimental pressure profiles → particularly evident for Ti.

- Ad-hoc models in TGLF to mimic fast ion stabilization do not help in improving the agreement with the experiment.

Can we do better with GENE-Tango?

ASDEX Upgrade 39230 @ t = 2.7 s - numerical setup

- GENE(global)-Tango simulations are performed with realistic electron-ion mass ratio, collisions, external ExB rotation.
- Magnetic equilibrium kept fixed to the one reconstructed via IDE.
- Cases analyzed: (i) no fast ions ES, (ii) no fast ions EM, (iii) with fast ions ES, (iv) with fast ions EM.

Case (iv): with fast ions EM

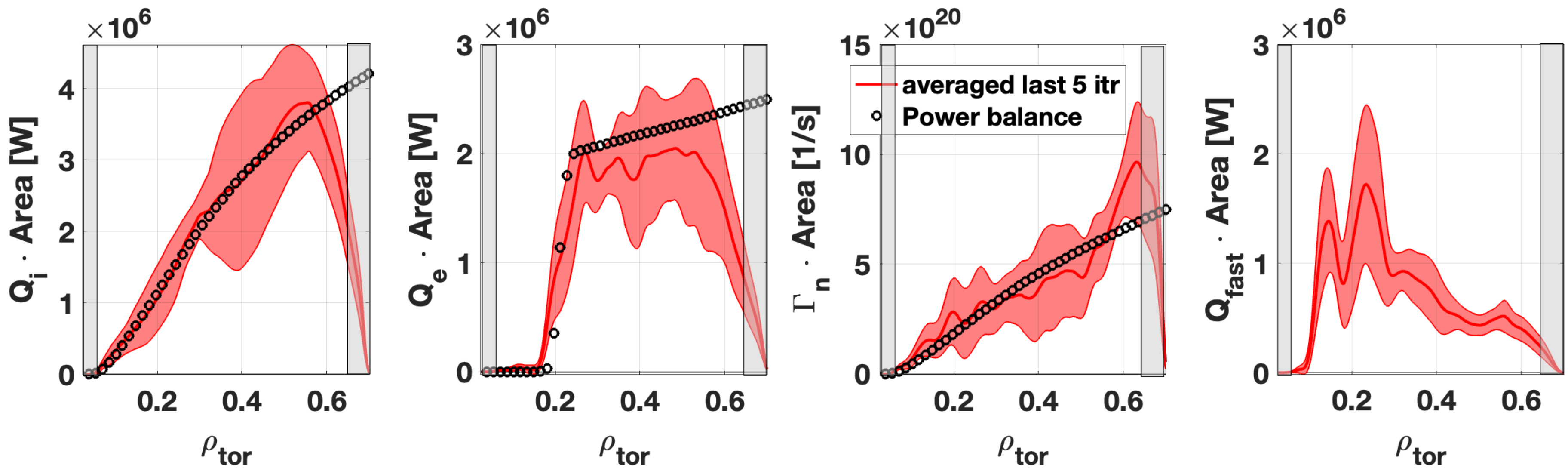

- Each case run until GENE turbulent fluxes match volume integral of injected heat and particle sources.

What is leading to the T_i peaking in the GENE-Tango simulations?

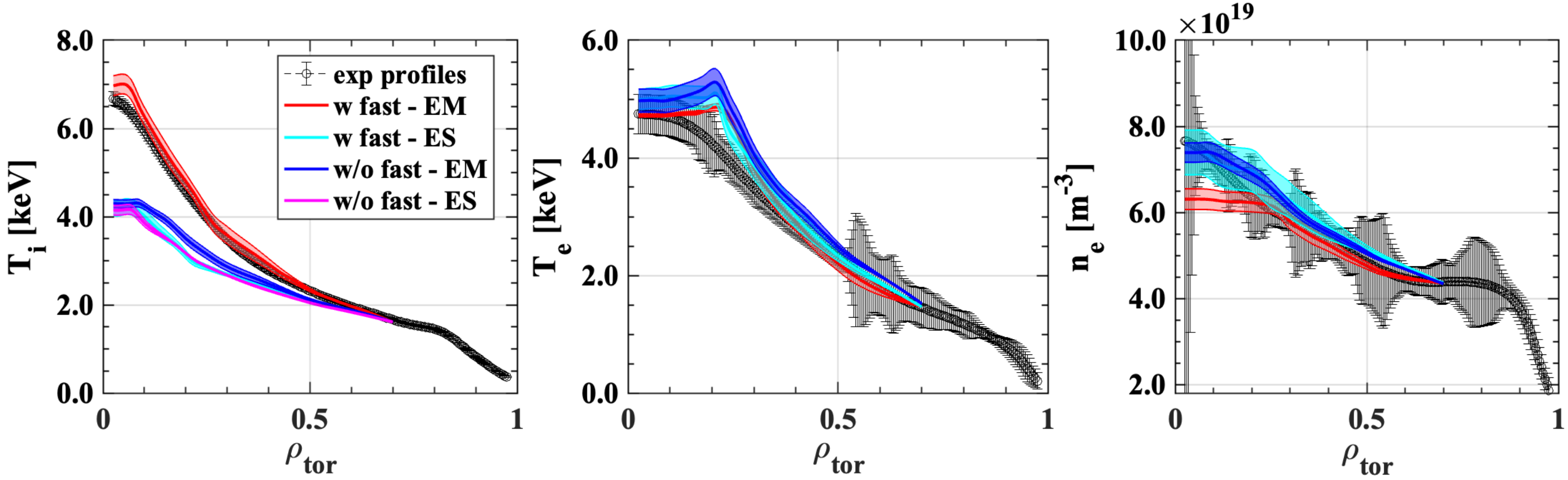

- Magnetic equilibrium itself (e.g., reversed shear, rational surfaces) cannot explain the increase on T_i on-axis.
- Electrostatic simulations (with or without fast ions) predict too much ITG transport → T_i stays at $\sim$ 4keV with negligible effects on T_e and density.
- Electromagnetic effects without fast ions lead to a mild peaking of T_i with minor impact on the on-axis value.
- Electromagnetic effects and fast particles are essential to reproduce experimental profiles.

Fast ion heat flux and rational surfaces

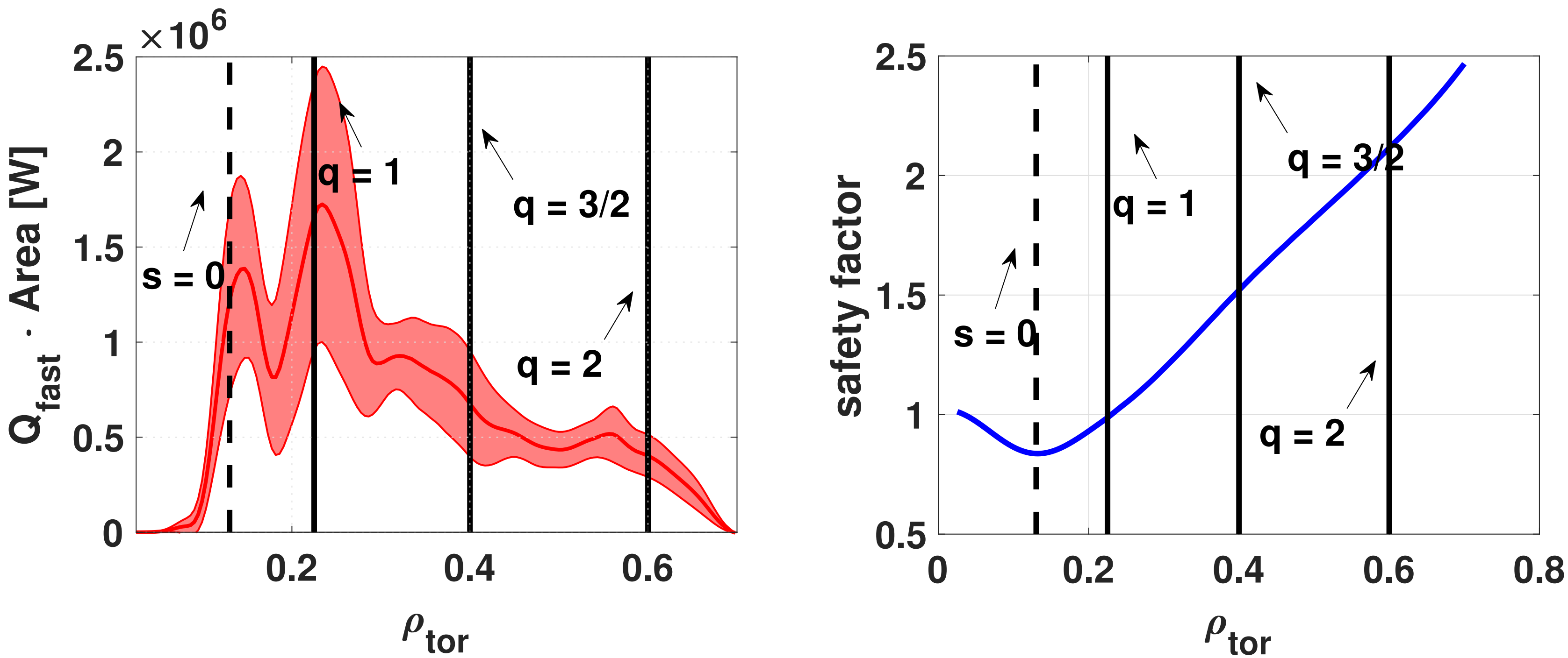

- Fast ion heat flux peaks at the rational surface $q = 1$ and $s = 0$.
- Other rational surfaces do not affect fast ion heat flux significantly - low fast ion density and temperature at $\rho_{tor} > 0.3$.

Fast ion heat flux and rational surfaces

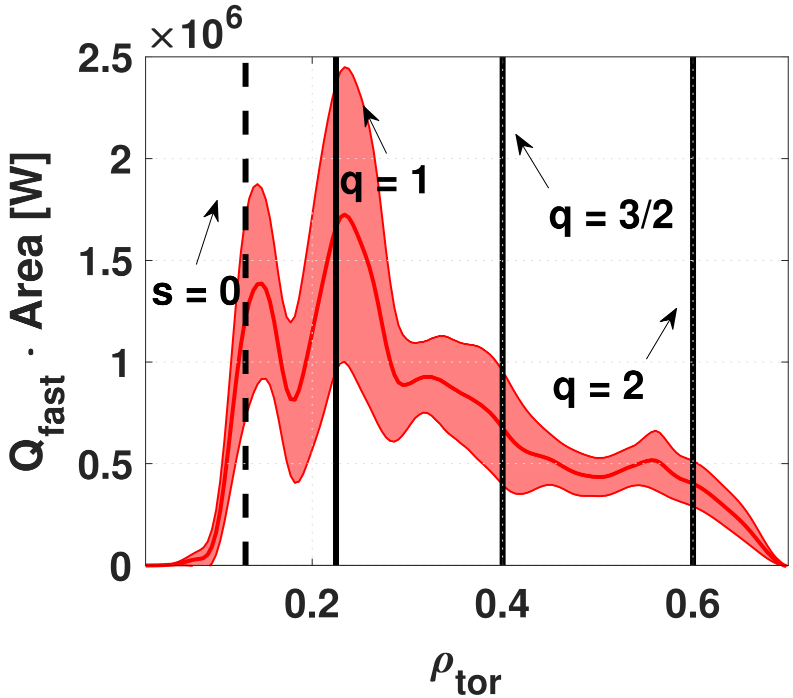

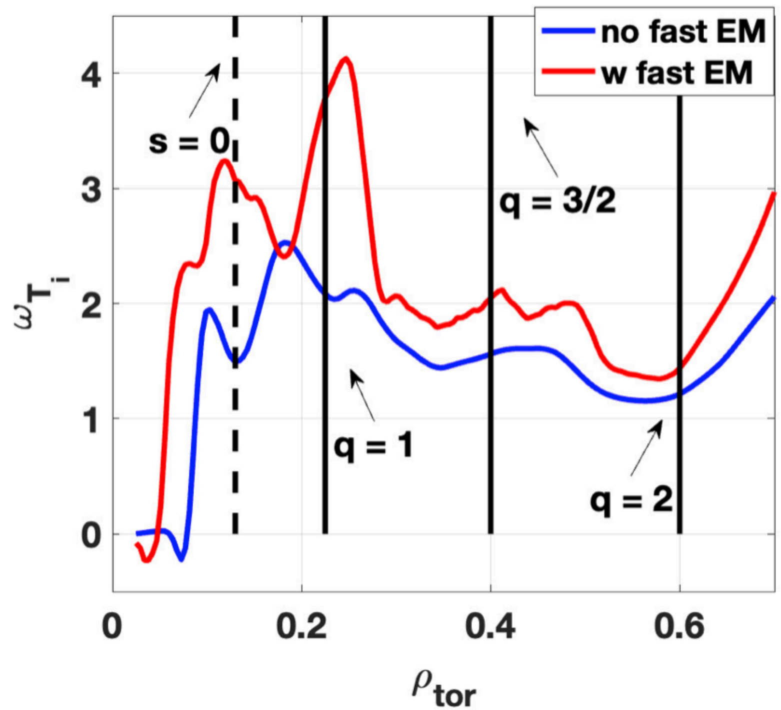

- The peaks of the energetic particle heat flux are strongly linked to the regions where the logarithmic temperature gradient increase.
- Simulation without fast ions - despite having same geometry - do not show clear improvements at $q = 1$ and $s = 0$.

Zonal structure generation by fast ion modes

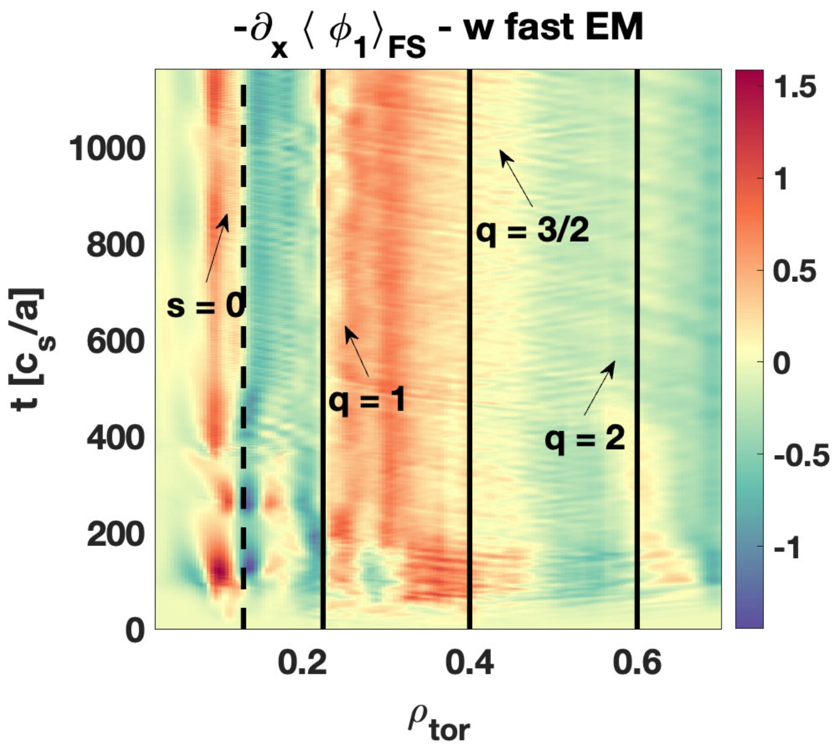

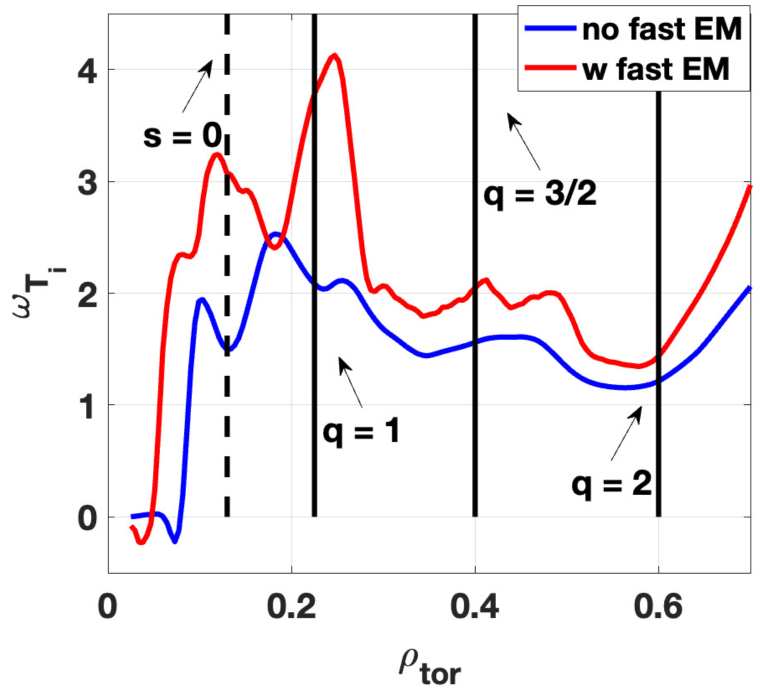

- Generation of flux-surface averaged radial electric field in proximity of $q = 1$ and $s = 0$.
- Simulation without fast ions - despite having same geometry - do not show clear improvements at $q = 1$ and $s = 0$ in ω_{T_i}.

Nonlinear spectra of electrostatic and $A_{1,\parallel}$ potential

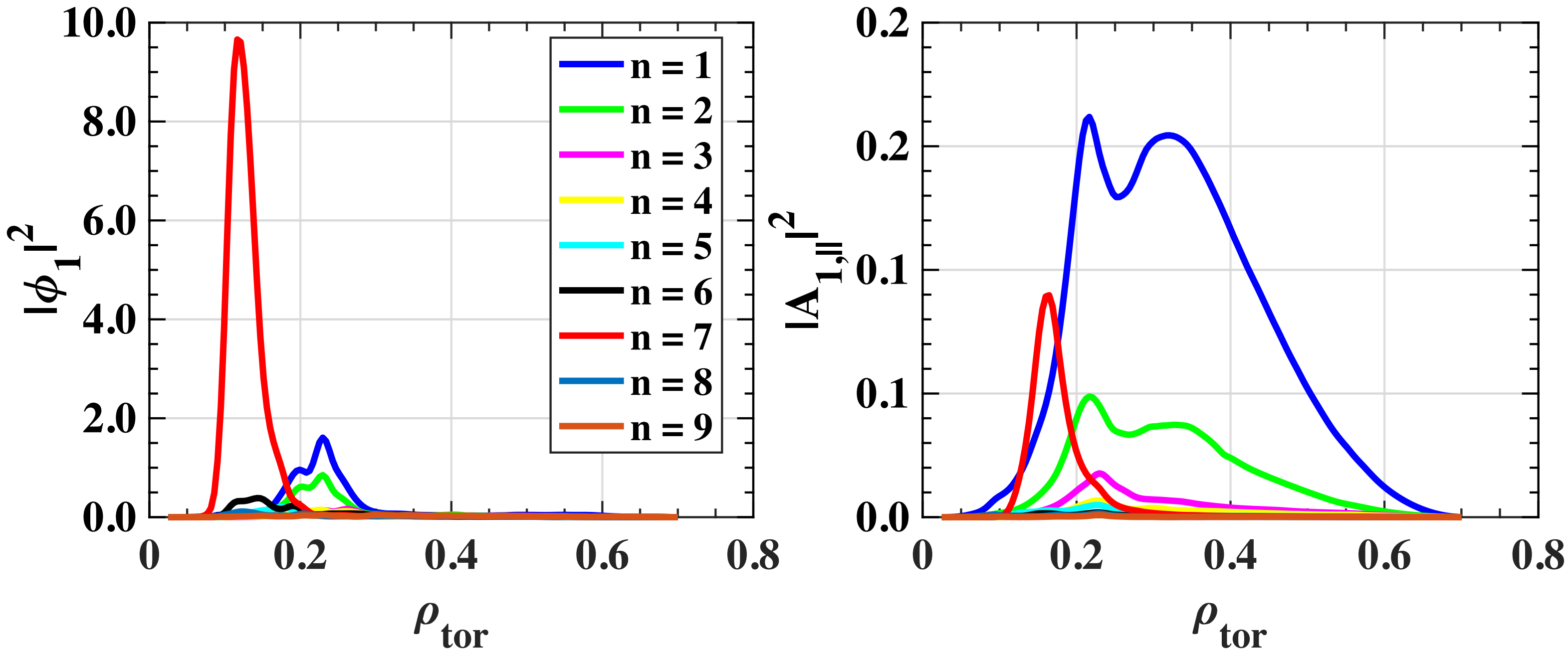

- The mode at $n = 7$, located at $s = 0$, exibits the largest amplitude in the electrostatic potential.
- The modes $n = [1,2]$ located at the rational surface $q = 1$, also have a large (and more global) contribution in both ϕ_1 and $A_{1,\parallel}$.

Nonlinear spectra of electrostatic potential

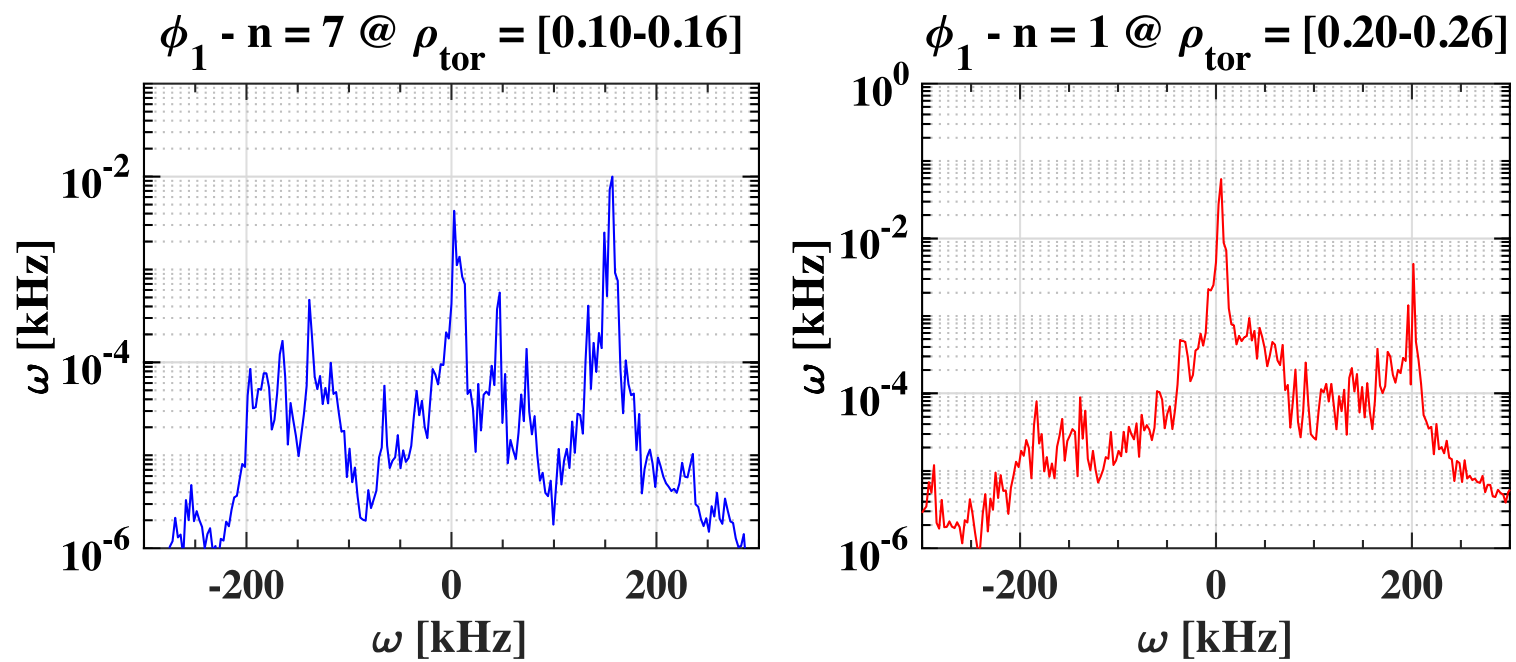

- In proximity of $s = 0$, electrostatic potential exhibits peaks at $\omega \approx 150$ kHz for $n = [7,14] \rightarrow$ compatible with linear observations.
- At the rational surface $q = 1$, electrostatic potential shows an high-frequency branch at $\omega \approx 200$ kHz for $n = [1 - 7]$.

Heat flux spectra

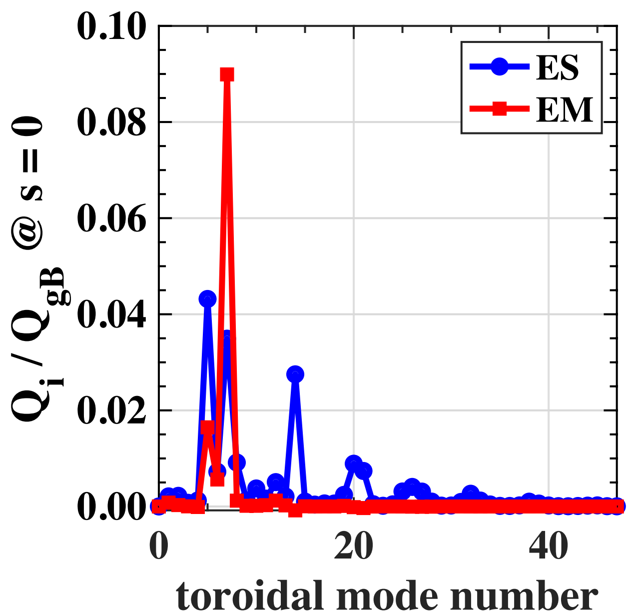

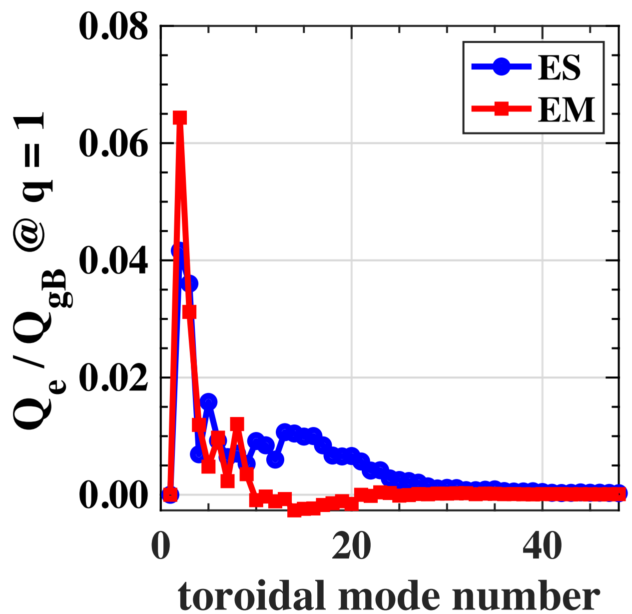

- The modes $n = [1,2,7]$ have a significant impact on the turbulent heat fluxes of each plasma species, as observed in the electron heat flux spectra.
- The dominant modes at $s = 0$ are characterized by $n = 7$ and its harmonics, while at $q = 1$ are the modes $n = [1,2]$, with large electromagnetic contributions, emphasizing their fundamental electromagnetic nature.

Linear stability analyses

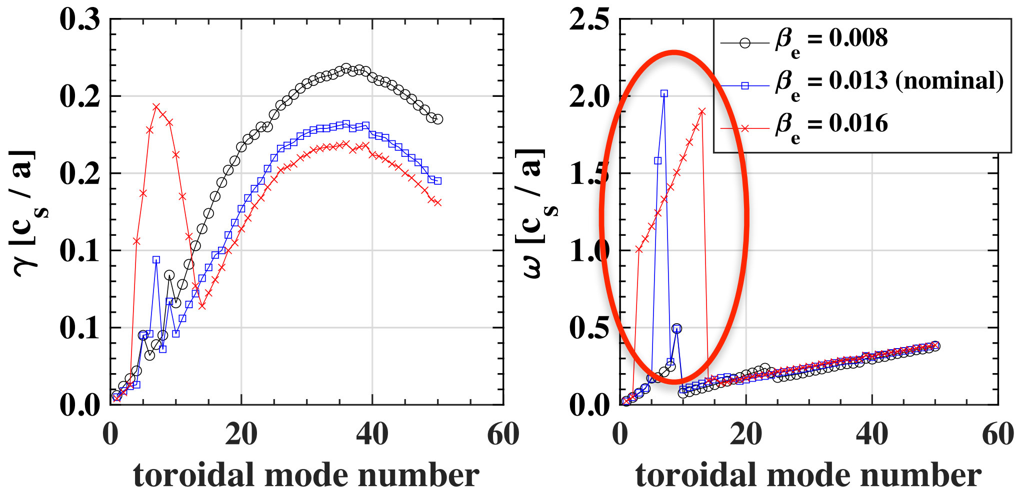

- Linear stability analyses were performed on the steady-state profiles to identify the most unstable modes.
- A mode transition to an electromagnetic high-frequency mode for $n = [6{,}7]$ was found for the steady-state profiles.
- No unstable electromagnetic high-frequency mode found in the linear simulations at $n = 1$.

Nonlinear cross-scale coupling

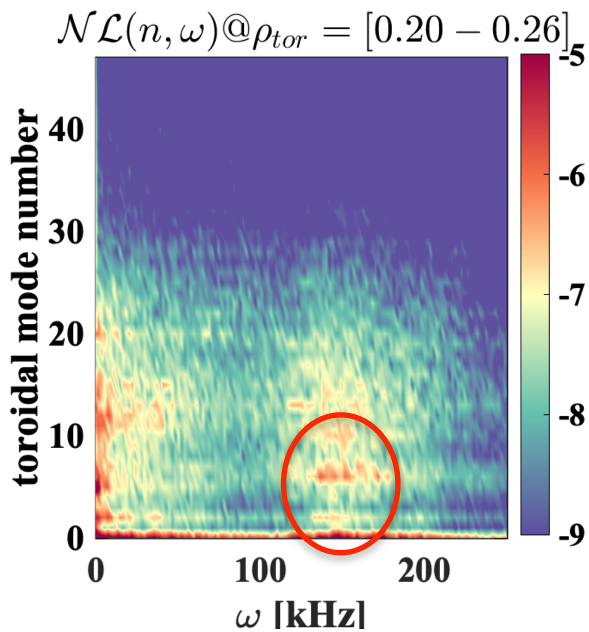

- Signatures of nonlinear cross-scale coupling between high-frequency modes with $n = [1{,}7]$ are observed at $s = 0$ and $q = 1$.
- These findings suggest that the linearly stable high-frequency mode at $q = 1$ could be nonlinearly excited via interaction with the unstable modes at $s = 0$.

Further destabilization of the high-frequency modes

- If the high-frequency modes get strongly unstable during the GENE-Tango iterations, thermal fluxes strongly increase → all profiles relax.

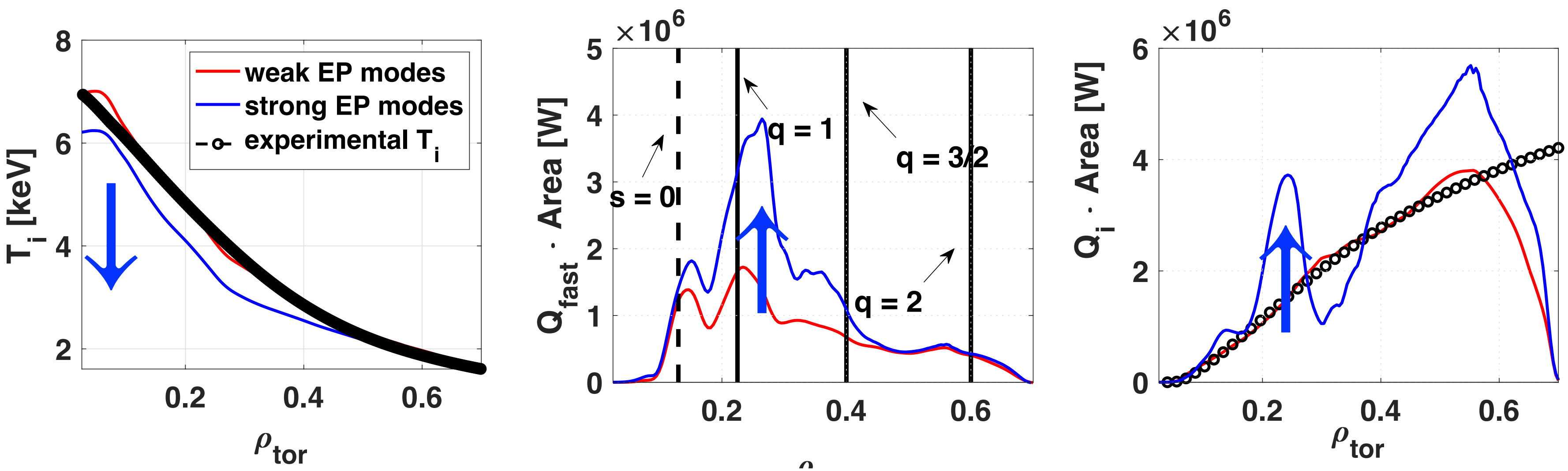

- Strongly unstable high-frequency modes cannot be sustained → turbulent fluxes increase.
- Tango reacts to the increases transport reducing the pressure gradients until <u>stabilizing or reducing the drive</u> of the high-frequency modes.

Conclusions:

- Electromagnetic GENE-Tango simulations with fast ions can reproduce the experimental plasma profiles of AUG discharge #39230 @ t = 2.7s.
- When fast particles are neglected in the GENE-Tango modelling all the simulations performed show a strong reduction of the T_i on-axis.
- These findings suggest that high-frequency modes might be responsible for the T_i peaking.
- Enhanced radial electric field at $s = 0$ observed in the electromagnetic GENE-Tango simulation with fast ions at the location of the high-frequency modes.
- When these high-frequency modes are strongly destabilized within the GENE-Tango iterations all turbulent fluxes increase.

Conclusions:

- Electromagnetic GENE-Tango simulations with fast ions can reproduce the experimental plasma profiles of AUG discharge #39230 @ t = 2.7s.
- When fast particles are neglected in the GENE-Tango modelling all the simulations performed show a strong reduction of the T_i on-axis.
- These findings suggest that high-frequency modes might be responsible for the T_i peaking.
- Enhanced radial electric field at $s = 0$ observed in the electromagnetic GENE-Tango simulation with fast ions at the location of the high-frequency modes.
- When these high-frequency modes are strongly destabilized within the GENE-Tango iterations all turbulent fluxes increase.

- **Caveat: this discharge has finshbone activity possibly not well modelled with GENE.**
- **Caveat: high-frequency modes are not observed experimentally.**

Conclusions:

- Electromagnetic GENE-Tango simulations with fast ions can reproduce the experimental plasma profiles of AUG discharge #39230 @ t = 2.7s.
- When fast particles are neglected in the GENE-Tango modelling all the simulations performed show a strong reduction of the T_i on-axis.
- These findings suggest that high-frequency modes might be responsible for the T_i peaking.
- Enhanced radial electric field at $s = 0$ observed in the electromagnetic GENE-Tango simulation with fast ions at the location of the high-frequency modes.
- When these high-frequency modes are strongly destabilized within the GENE-Tango iterations all turbulent fluxes increase.

Thank you for your attention!

Backup slides:

Comparison with GENE flux-tube simulations

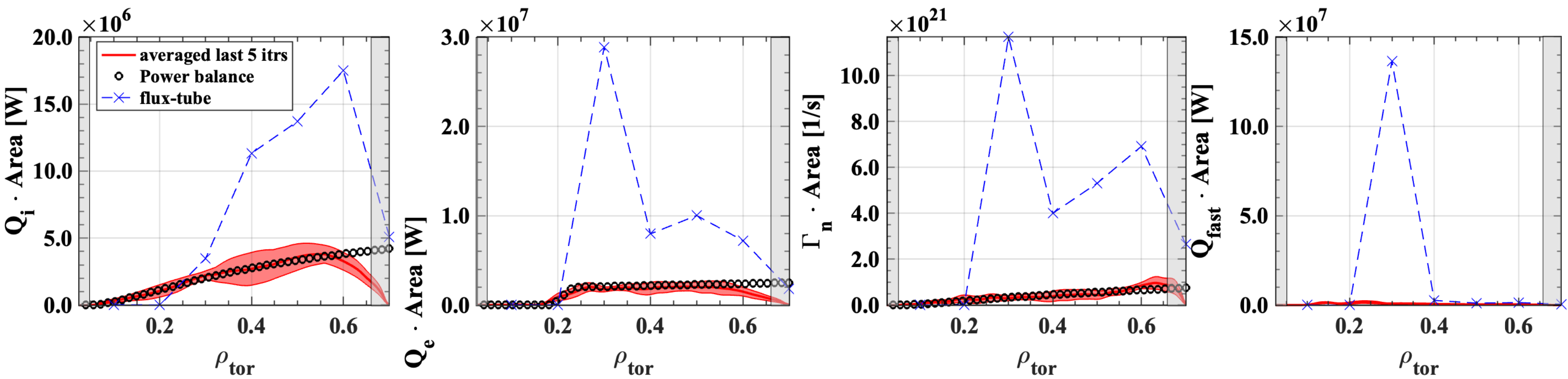

- Flux-tube GENE simulations are performed at seven radial locations.
- Large turbulent fluxes observed in the flux-tube simulations which are not compatible with power balance.
- Unstable high-frequency modes cannot be sustained in flux-tube simulations → profile will likely flatten until reducing plasma beta to stabilize these high-frequency modes.

Nonlinear electromagnetic fast ion turbulence suppression

Coupling to marginally-stable fast ion modes [A. Di Siena et al. NF 2019, JPP 2021]

- Fast particles provide linearly stable modes destabilised nonlinearly.
- Energy redistribution from thermal to fast ion-driven modes → depleting the energy content of the turbulence.
- When the fast ion drive is sufficiently large, fast particle modes interact with zonal flow.
- Direct impact of zonal flows on ITGs, strongly suppressing heat/particle fluxes.

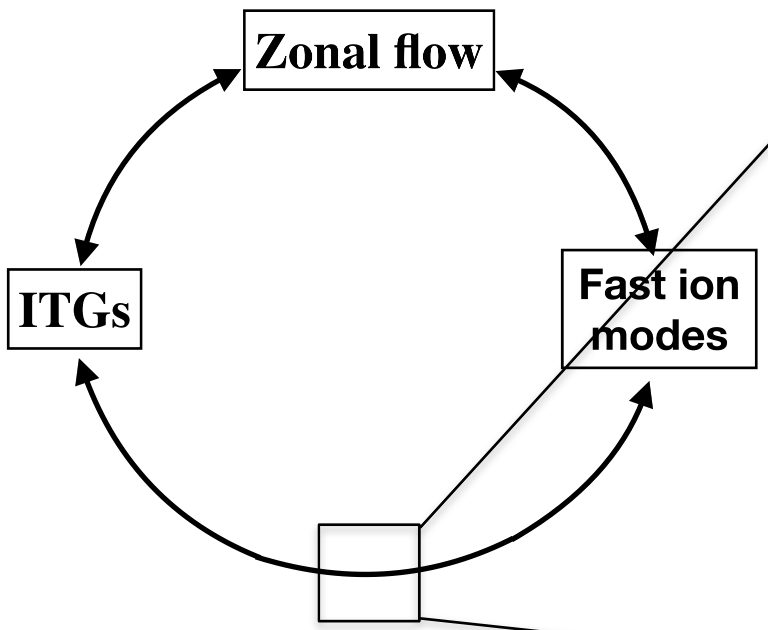

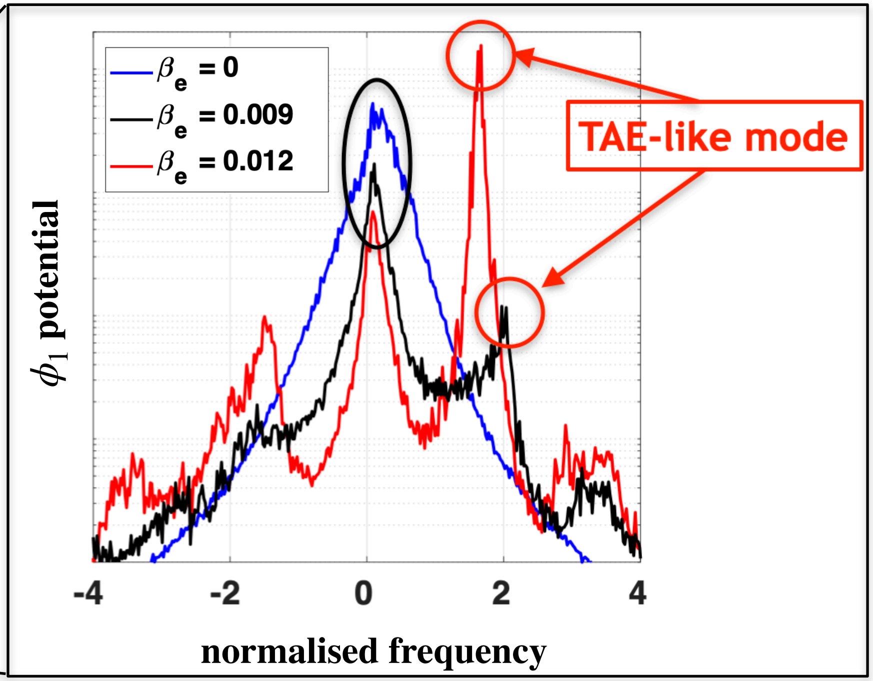

Nonlinear electromagnetic fast ion turbulence suppression

Coupling to marginally-stable fast ion modes [A. Di Siena et al. NF 2019, JPP 2021]

- Fast particles provide linearly stable modes destabilised nonlinearly.
- Energy redistribution from thermal to fast ion-driven modes → depleting the energy content of the turbulence.
- When the fast ion drive is sufficiently large, fast particle modes interact with zonal flow.
- Direct impact of zonal flows on ITGs, strongly suppressing heat/particle fluxes.

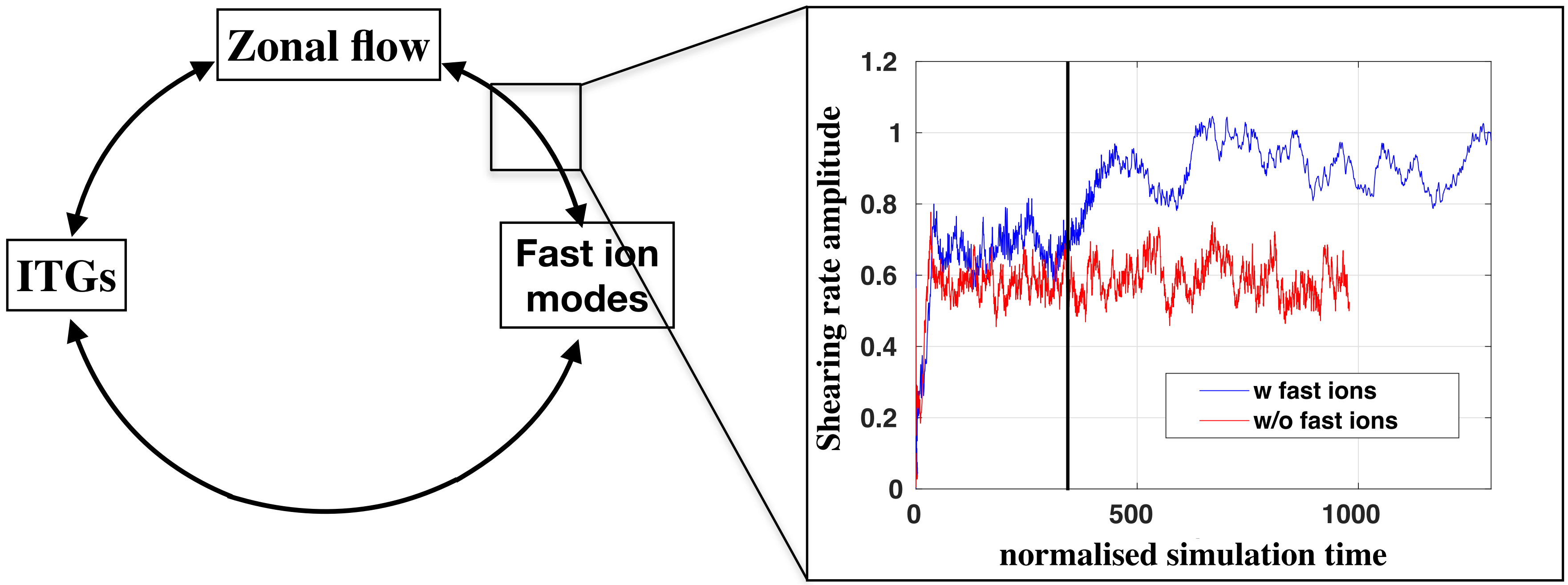

Motivation

Destabilising fast ion effects

- Large fast particle pressure/pressure gradients may drive unstable fast ion modes → large increase in overall turbulence fluxes [J. Citrin et al. PPCF 2015, J. Garcia et al. NF 2015]

J. Citrin et al. PPCF 2015

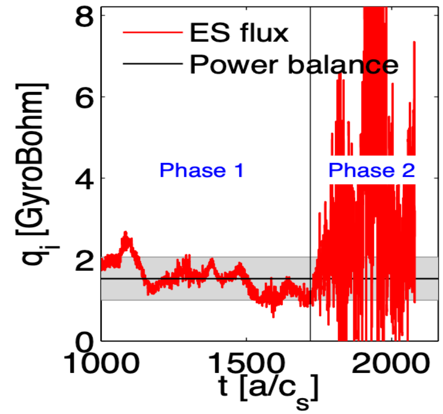

Stabilising fast ion effects

- Dilution of thermal ITG drive [G. Tardini et al. NF 2007, C. Angioni et al. PoP 2008, J. Wilkie et al. JPP 2015]
- Increase geometrical stabilisation through Shafranov shift [C. Bourdelle et al. NF 2005]
- ITG - fast ion drift resonance [A. Di Siena et al. NF 2018, PoP 2019, PRL 2020, PRL 2021]
- Nonlinear coupling between marginally stable fast ion modes, ITG turbulence and zonal flow [J. Citrin et al. PRL 2013, J. Garcia et al. NF 2015, A. Di Siena et al. NF 2019, JPP 2021]

C. Angioni et al. PoP 2018

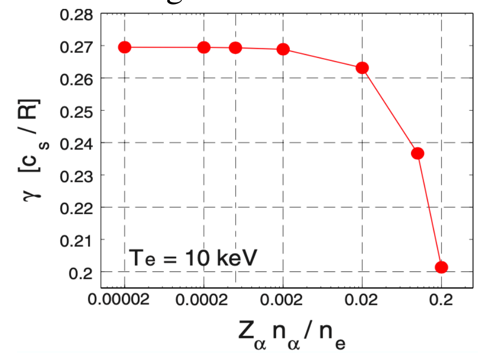

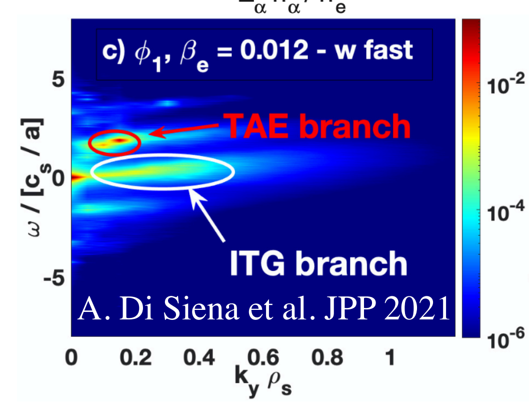

Nonlinear electromagnetic fast ion turbulence suppression (3)

Coupling to marginally-stable fast ion modes [A. Di Siena et al. NF 2019, JPP 2021]

- Similar results are observed in an increasing number of experimental scenarios where substantial turbulent stabilisation is attributed to energetic particles:
  - JET L-mode #73224 with both NBI and ICRH.
  - AUG H-mode #31563 with ICRH.
  - AUG H-mode #32305 with NBI.

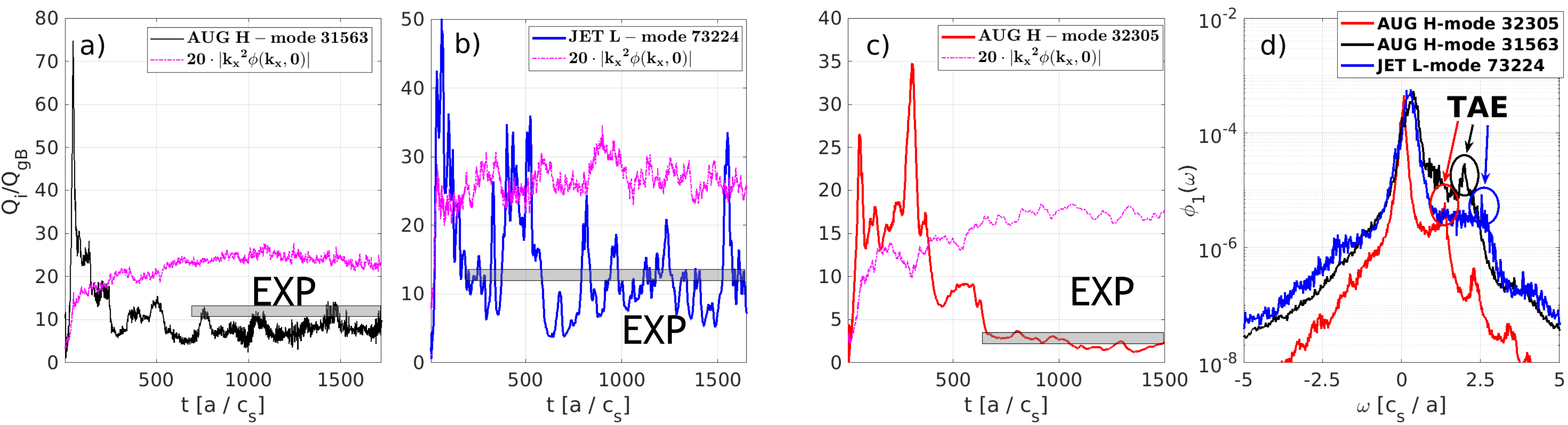

Nonlinear spectra of electrostatic potential

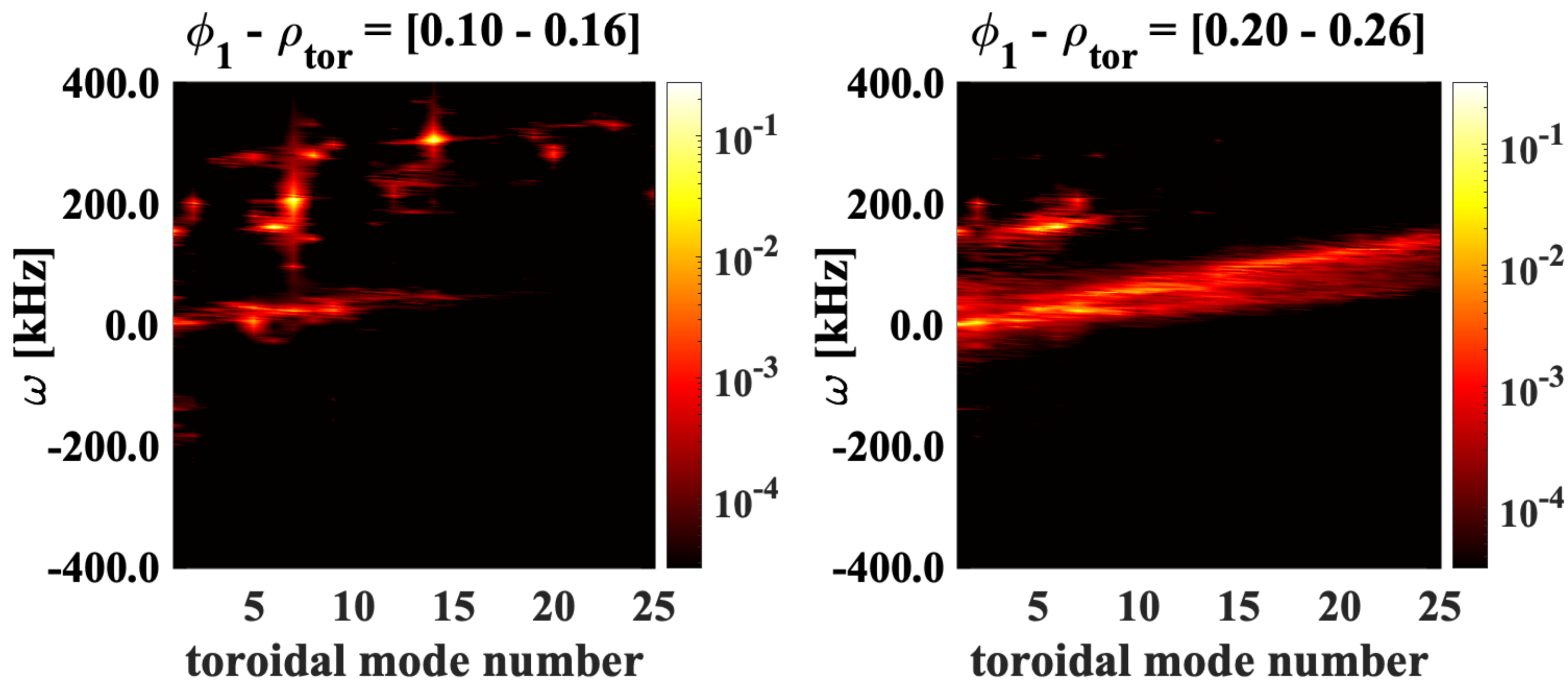

- In proximity of $s = 0$, electrostatic potential exhibits peaks at $\omega \approx [200 - 300]$ kHz for $n = [7{,}14] \rightarrow$ compatible with linear observations.
- At the rational surface $q = 1$, electrostatic potential shows an high-frequency branch at $\omega \approx 200$ kHz for $n = [1 - 7]$.

Transport solver Tango: basic equations

1D transport equation

- Macroscopic profiles are constant on magnetic flux surfaces

$$\frac{3}{2}A\frac{\partial p}{\partial t} + \frac{\partial}{\partial x}AQ = AS$$

J. Parker et al. NF 2018
A. Shestakov et al. JCP 2003

A: Area flux-surface

Q = $\langle Q \cdot \nabla x \rangle$: Turbulent fluxes

S: Sources

- subscript ***m***: transport time step index; ***l***: iteration index within a time step

$$\frac{3}{2}A\frac{p_{m,l} - p_{m-1}}{\Delta t} = \frac{\partial}{\partial x}(AQ_{m,l}[p_{m,l}]) + AS_m$$

- Turbulent fluxes taken as **time-average quantities** over many turbulent time steps (in the saturated phase) $\Delta\tilde{t}$ and the pressure profile is evolved by the macroscopic time step Δt

Transport solver Tango: basic equations

1D transport equation

- Macroscopic profiles are constant on magnetic flux surfaces

J. Parker et al. NF 2018
A. Shestakov et al. JCP 2003

$$\frac{3}{2}A\frac{\partial p}{\partial t} + \frac{\partial}{\partial x}AQ = AS$$

A: Area flux-surface

$Q = \langle Q \cdot \nabla x \rangle$: Turbulent fluxes

S: Sources

- subscript ***m***: transport time step index; ***l***: iteration index within a time step

$$\frac{3}{2}A\frac{p_{m,l} - p_{m-1}}{\Delta t} = \frac{\partial}{\partial x}(AQ_{m,l}[p_{m,l}]) + AS_m$$

- Q is the sum of diffusive and convective contributions

$$Q_{m,l} = -D_{m,l-1}\frac{\partial p_{m,l}}{\partial x} + c_{m,l-1}p_{m,l}$$

Transport solver Tango: basic equations

- There is freedom in the splitting of the turbulent flux Q between D and c

$$D_{m,l-1} = -\frac{\theta_{l-1} Q[p_{m,l-1}]}{\frac{\partial p_{m,l-1}}{\partial x}} \qquad c_{m,l-1} = \frac{(1-\theta_{l-1}) Q[p_{m,l-1}]}{p_{m,l-1}}$$

- θ denotes the nature of the turbulent fluxes, i.e. diffusive and/or convective, assuming plasma turbulence mainly diffusive $\rightarrow \theta \sim 1$
- Diffusion coefficients depending on $\partial p_{m,l-1}/\partial x$ makes the iteration numerically unstable. It is stabilised by adding the relaxation coefficient α to D and c

$$\bar{Q}_{m,l-1} = \alpha Q[\hat{p}_{m,l-1}] + (1-\alpha)\bar{Q}_{m,l-2}$$

$$\bar{p}_{m,l-1} = \alpha p_{m,l-1} + (1-\alpha)\bar{p}_{m,l-2}$$

Transport solver Tango: basic equations

- There is freedom in the splitting of the turbulent flux Q between D and c

$$D_{m,l-1} = -\frac{\theta_{l-1}\bar{Q}[p_{m,l-1}]}{\frac{\partial \bar{p}_{m,l-1}}{\partial x}} \qquad c_{m,l-1} = \frac{(1-\theta_{l-1})\bar{Q}[p_{m,l-1}]}{\bar{p}_{m,l-1}}$$

- θ denotes the nature of the turbulent fluxes, i.e. diffusive and/or convective, assuming plasma turbulence mainly diffusive → $\theta \sim 1$
- Diffusion coefficients depending on $\partial p_{m,l-1}/\partial x$ makes the iteration numerically unstable. It is stabilised by adding the relaxation coefficient α to D and c

$$\bar{Q}_{m,l-1} = \alpha Q[\hat{p}_{m,l-1}] + (1-\alpha)\bar{Q}_{m,l-2}$$

$$\bar{p}_{m,l-1} = \alpha p_{m,l-1} + (1-\alpha)\bar{p}_{m,l-2}$$

Transport solver Tango: basic equations

- Tango solves iteration equation within an implicit timestep advance of a transport equation: nonlinear equation for the time-advanced (backward Euler step)

$$\frac{3}{2}A\frac{p_{m,l}-p_{m-1}}{\Delta t} = \frac{\partial}{\partial x}\left(AD_{m,l-1}\frac{\partial p_{m,l}}{\partial x} - Ac_{m,l-1}p_{m,l}\right) + AS$$

- Each coefficient is evaluated at the previous iterate ***l*-1** and the transport equation is linear in the unknown $p_{m,l}$

$$M_{m,l-1}p_{m,l} = g$$

***l*-1 terms** → $M_{m,l-1}$

Sources + terms p_{m-1} → g

- When the iteration in ***l*** converges, the representation for the flux (right-hand side) is equal to the actual turbulent flux Q (left-hand side)

$$Q_{m,l} = \int dV(P_{ICRH} + P_{NBI} + \ldots)$$